Exposure Characterization of Ultrafine Particles From the Blast Furnace Process in a Steelmaking Plant

Xiangjing Gao
Department of Occupational Health and Radiation Protection, Zhejiang Provincial Center for Disease Control and Prevention, Hangzhou 310051, Zhejiang, China https://orcid.org/0000-0002-3551-8569

Hua Zou
Department of Occupational Health and Radiation Protection, Zhejiang Provincial Center for Disease Control and Prevention, Hangzhou 310051, Zhejiang, China

Qunli Wang
Ningbo municipalcenter for disease control and prevention, Ningbo 315010, Zhejiang, China

Zanrong Zhou
Department of Occupational Health and Radiation Protection, Zhejiang Provincial Center for Disease Control and Prevention, Hangzhou 310051, Zhejiang, China

Weiming Yuan
Department of Occupational Health and Radiation Protection, Zhejiang Provincial Center for Disease Control and Prevention, Hangzhou 310051, Zhejiang, China

Yuqing Luan
Department of Occupational Health and Radiation Protection, Zhejiang Provincial Center for Disease Control and Prevention, Hangzhou 310051, Zhejiang, China

Changjian Quan
Department of Occupational Health and Radiation Protection, Zhejiang Provincial Center for Disease Control and Prevention, Hangzhou 310051, Zhejiang, China

Meibian Zhang (mbzhang@cdc.zj.cn)
Department of Occupational Health and Radiation Protection, Zhejiang Provincial Center for Disease Control and Prevention, Hangzhou 310051, Zhejiang, China https://orcid.org/0000-0002-6839-737X

Shichuan Tang
Beijing Municipal Institute of Labor Protection, Beijing 100054, China

---

Research

Keywords: ultrafine particles, occupational exposure, number concentration, surface concentration, steelmaking

Posted Date: August 14th, 2020

DOI: https://doi.org/10.21203/rs.3.rs-54690/v1

Abstract

Background: Information regarding the exposure characteristics of ultrafine particles generated by working activities in the steelmaking industry is very limited. This study aimed to investigate the exposure characteristics of ultrafine particles from the blast furnace process in a steelmaking industry.

Methods: The morphology of particles, their elemental compositions, temporal variations in particle concentrations (e.g., total number concentration (NC), total respirable mass concentration (MC), surface area concentration (SAC)), personal exposure level, and the size distributions by number were measured. The relationships among total NC, total respirable MC, and SAC were determined by analyzing the concentration ratios (CR), correlation coefficients (CC), and the consistency of temporal variations in particle concentrations.

Results: The particles collected from the blast furnace process presented as irregular agglomerates, and the predominant elements were O, Al, and Si. The total NC, total respirable MC, and SAC increased after working activity started and decreased gradually to background levels after the operation stopped. The median, mean, geometric mean, and modal sizes of particles remained relatively stable during working activities, ranging from 20 to 50 nm. Size distribution by number showed that the sizes of particles released from the slag releasing location were mainly gathered at 10.4 and 40 nm. The highest numbers appeared at 10.4 nm and 40 nm, which reached 3×10^6 pt/cm^3. Particles ranging 100–469 nm were less than 8×10^5 pt/cm^3, while particles with sizes larger than 374 nm were less than 2×10^4 pt/cm^3. There was a good correlation between the total NC, SAC, and respirable MC. The order of CC for these three parameters was $R_{\text{total NC and SAC}}$ ($r = 0.681$) > $R_{\text{SAC and respirable MC}}$ (0.456) > $R_{\text{total NC and respirable MC}}$ (0.424).

Conclusions: These findings indicate that working activities generated high levels of ultrafine particles. The ultrafine particle concentrations exhibited activity-related and periodic variations. The total NC and SAC were more appropriate metrics for characterizing ultrafine particles at the slag releasing location than total respirable MC. This study provides baseline data on the exposure characteristics of ultrafine particles during the blast furnace process.

Background

The steelmaking industry contributes significantly to the world's industrial economy, with a total estimated worth of $900 billion per year[1]. Materials used in almost everything today, such as housing, transportation, energy production, food containers, and water supply pipes, either come from steel or are manufactured using steel equipment[1]. In developing countries, there is an increasing demand for steel production for industrialization and modernization. China has become the largest steel producer in the world[2] and the volume of crude steel production has rapidly increased to 928.3 million tons in 2018[3]. With the increasing use of steel production in our daily life, its negative impact on the air quality during manufacturing processes is becoming prominent[4-6]. The amount of dust released from steelmaking

industries accounts for 27% of China's dust emissions, which are estimated at 2–5 million tons per year[7, 8]. Melting, blast furnaces, and other hot processes are known to be significant contributors to dust emission in steelmaking plants[9]. Ultrafine particles account for a large proportion (more than 50%) of the dust released as a result of these hot processes[10].

Exposure to ultrafine particles or their aggregates (fine particles) may result in adverse health problems for humans, such as acute respiratory illness, chronic coughing, and a reduction in lung function[11, 12]. Ultrafine particles produced by steelmaking have attracted public attention. There have been many studies on the exposure to these ultrafine particles. For example, the concentration of volatile organic compounds (VOCs) in outdoor air samples from the integrated steelmaking industry has been analyzed [13]. Typical hazardous air pollutants, size-segregated particulate matter (TSP/PM_{10}/$PM_{2.5}$), gaseous pollutants (SO_2, NO_x, CO), and heavy metals (Pb, Cd, Hg, As, Cr, Ni, etc.) from the steelmaking industry in China exhibited characteristic temporal and spatial variations or trends[14]. The composition of the various size fractions of cast house dust and the chemical composition and source apportionment of particles near steelmaking industrial areas in China was investigated[15, 16]. Fan Zhen et al. investigated the morphology, chemical composition, mass concentration (MC), and number concentration (NC) of $PM_{2.5}$ in outdoor air samples released from a blast furnace, and found that the size of particles was mainly below 1.0 μm[17].

The above studies revealed the compositions and outdoor concentrations of ultrafine particles released from manufacturing processes in the steelmaking industry, which provides an idea for investigating the occupational exposure of indoor ultrafine particles in the steelmaking industry. Until now, there have been few studies on the occupational exposure characteristics of indoor ultrafine particles in steelmaking plants. Järvelä et al. described workers' exposure to fine and ultrafine particles in the production chain of ferrochromium and stainless-steel during sintering, ferrochromium smelting, stainless steel melting, and hot and cold rolling operations[18]. The authors characterized the MC, NC, and size distribution[18], but missed the most important producing-particle source, e.g. the process of blast furnace, and did not mention particle nature and temporal variations in particle concentrations or size distribution. The temporal variations in particle concentrations, which cover one full period of working activity, should be considered because there might be multiple hazardous factors existing in the workplace. Moreover, temporal variations in size distribution should be taken into account as it might be affected by the agglomeration of primary particles[19]. Further, the particle nature, which can provide information on the chemical compositionsassociated with the potential health risk of workers, should be assessed using qualitative and quantitative approaches. Therefore, to bridge the above research gap, it is necessary to investigate the exposure characteristics of indoor ultrafine particles from the blast furnace process, including particle nature, temporal variations in particle concentrations, and size distribution.

The aim of this study was to investigate the exposure characteristics of indoor ultrafine particles from the blast furnace process in the steelmaking industry from the following three aspects: (1) the particle nature (morphology and elemental compositions); (2) the temporal variation in total concentrations of particles

(namely, total NC, total respirable MC, personal NC, and SAC); and (3) the temporal variation in size distributions by number concentration. This study will provide a deeper understanding of the occupational exposure characteristics of indoor ultrafine particles in the steelmaking industry to reduce the exposure risk of workers by taking effective control measures.

Methods

Description of workplace

A blast furnace position in a steelmaking plant in the Zhejiang Province of East China was selected for field investigation. In this plant, the major production process is described as follows: (1) coking: coal is coked through a coke oven; (2) blast furnace: solid raw materials such as iron ore, coke, and flux agents are fed into a blast furnace in batches by a top charging device based on the specified batch ratio. The iron ore is gradually reduced and melted into iron and slag during the process of falling. Liquid iron and slag are gathered in a furnace belly, and periodically released from the iron and slag mouth; (3) converter: the liquid iron from the blast furnace and scrap steel is heated in an oven; (4) steel rolling: the molten steel is transported to a turntable through steel drums, and is then divided into several strands through a molten steel distributor and injected into casting molds. Finally, solidified shells are formed after cooling and solidifying. Among these processes, the blast furnace, which comprises a continuous melting process and periodical slag releasing operations, is a potential source for the release of ultrafine particles.

Monitoring and sampling systems

Table 1 shows the monitoring and sampling systems. The real-time system monitored the total NC, total respirable MC, surface area concentration (SAC), and size distribution by number. The total NC was determined using a P-TRAK ultrafine particle counter (Model 8525; TSI, Shoreview, MN). It is a portable condensation particle counter (CPC) for measuring the NC of ultrafine particles[20, 21]. The personal NC was measured using a Diffusion Size Classifier Miniature (DiSCmini), which can measure the number and average size of nanoparticles (< approximately 0.7 μm) in air by testing the electrical current of charged aerosols with a sensitive electrometer. The total respirable MC was tested using a real-time aerosol monitor (DustTrak 8533, TSI, Shoreview, MN), a luggable laser-scattering photometer, which can measure particles ranging from 100 nm to 1000 nm. The alveolar deposition mode of SAC was determined using a surface area monitor (Aero TrakTM 9000, TSI, USA). A suite of aerosol instruments covering the size range from 10.4 nm to 10 μm are used to capture the particle size distribution and number concentration, including the scanning mobility particle sizer (SMPS, Model 3034, TSI, USA), which consists of a differential mobility analyzer (DMA) and a CPC, and optical particle sizer (OPS, Model 3330, TSI, USA). Several types of particle sizes were obtained from the data output of the SMPS and OPS, including the mode size, median size, arithmetic mean size, and geometric mean size.

A membrane-based sampling system was used to collect ultrafine particles to analyze their morphology and elemental compositions. Ultrafine particles were collected using a cascade impactor (Nano-MOUDI,

125A, MSP, USA). The impactor comprised thirteen stages, corresponding to cut sizes of 10000, 5600, 3200, 1800, 1000, 560, 320, 180, 100, 56, 32, 18, and 10 nm. The morphology of ultrafine particles collected at the 13th stage was analyzed using a scanning electron microscopy (SEM, S4800; Hitachi, Tokyo, Japan), while elemental compositions were analyzed using an energy-dispersive X-ray spectroscopy (EDX, S4800; Hitachi).

Table 1. Monitoring and sampling system for measuring particles

Monitoring types	Exposure metrics	Instruments	Particle sizes (nm)	Measuring range	Sampling rate (L/min)	Log interval (min)
Real-time monitoring	Total NC	P-TRAK 8525 (TSI, USA)	20-1000	0-500000 particles/cm^3 (pt/cm^3)	0.1 L min^{-1}	1min
	Personal NC	DiSCmini (TESTO, Germany)	<700	0-5000000 pt/cm^3	1.0 L min^{-1}	1min
	Total respirable MC	Dust Trak 8533 (TSI, USA)	100-1000	0.01-150 mg/m^3	3 L min^{-1}	1min
	SAC	Aero TrakTM 9000 (TSI, USA)	10-1000	1-10000 $\mu m^2/cm^3$	2.5 L min^{-1}	1min
	Size distribution by number	SMPS 3034 (TSI, USA)	10-487	1-2.4×10^6 pt/cm^3	1.0 L min^{-1}	3min
		OPS 3330 (TSI, USA)	300-10000	0-3000 pt/cm^3	1.0 L min^{-1}	1min
Membrane-based sampling	Morphology	SEM S4800 (Hitachi, Japan)	10-10000	-	-	-
	Elemental composition	EDX (Hitachi, Japan)	10-10000	-	-	-

Sampling and testing strategies

The sampling process was performed in August 2019. After field investigation, concentration screening by the CPC was conducted to identify the potential source of particle emission, as our previous study reported[21, 22]. The sampling protocol was as follows: (i) background measurements: background particles from the atmosphere were collected 45 m from the blast furnace, as shown in Figure 1 (Location). No incidental particle sources were present in the workshop during the sampling period, such

as vacuum pumps, heating units, diesel-powered forklifts, or welding systems. (ii) area sampling based on activity: the sampling locations were selected based on the information gathered and the walkthrough survey, considering several factors. These included air movement and currents, work tasks, temperature of the heat source, and whether the location could allow for the placement of large instruments without normal work activities being affected. In this study, both blast furnace and slag releasing were substantial sources of ultrafine particles. However, the temperature of the blast furnace was too high to place the testing instruments close to it. Hence, the slag releasing was selected as the sampling location. The sampling location was selected beside the slag ditch, as shown in Figure 1 (Location □). Area sampling was performed based on the changes in the working period and working activity and covered at least one complete work flow. Sampling was performed 1.3 m above the floor and close to the operating position potentially exposed to the ultrafine particles. (□) Personal sampling: The operating worker at the blast furnace position was selected as the subject, and the sampling period covered one complete work flow. The sampler was placed near the snout, approximately 30 cm away from the breathing zone.

Statistical analysis

One-way analysis of variance (ANOVA), followed by the Dunnett's T3 multiple comparison method, was used to analyze the differences in the total NC, total respirable MC, and SAC between the sampling location and background. Pearson correlation was applied to analyze the relationships among different exposure metrics (total NC, total respirable MC, and SAC). The total NC, total respirable MC, and SAC were corrected using background concentrations to obtain the concentration ratios (CR) (sampling location vs. background), which reflected the degree of ultrafine particles released from the source.

Results

Mean concentrations and mode sizes of particles

The mean concentrations and mode sizes of particles at the slag releasing location and background are listed in Table 2. The mean total NC, SAC, and total respirable MC at the slag releasing were 5.33 ± 1.61 × 10^4 pt/cm^3, 2236.43 ± 2.21 $\mu m^2/cm^3$, and 0.31 ± 0.12 mg/m^3, respectively, which were significantly higher than those of the background particles ($p < 0.01$). The mean total NC of personal sampling during the working activity period was95.39 ± 68.70pt/cm^3, which was much higher than the slag releasing measured with P-TRAK. The mode sizes of the slag releasing and background were 26.08 ± 10.88 nm and 58.28 ± 13.87 nm, respectively. The mode size of personal sampling was 28.48 ± 4.53 measured with DiSCmini during the working activity period, which was similar to that of slag releasing (26.08 ± 10.88) measured with SMPS. The mode size of personal sampling during the non-activity period (86.50 ± 9.40) was larger than the background (58.28 ± 13.87).

Table 2. Mean concentrations and mode size of ultrafine particles at different sampling sites

Metrics	Background (n=60)		Slag releasing (n=50)		Personal sampling during working activity period (n=60)	Personal sampling during non-activity period (n=50)
	Mean±SD	CR	Mean±SD	CR		
Total NC (10^4 pt/cm^3)	2.11±0.67	1.00	6.05±1.82	2.87	95.39±68.70	2.21±0.60
Total respirable MC (mg/m^3)	0.09±0.01	1.00	0.20±0.02	2.22	-	-
SAC (μm^2/cm^3)	301.98±18.79	1.00	1628.07±740.11	5.39	-	-
Mode size (nm)	58.28±13.87	-	26.08±10.88	-	28.48±4.53	86.50±9.40

Morphology and elemental composition of ultrafine particles

Figure 2 shows the morphology of particles collected from the slag releasing (a) and background (b) locations, which exhibited different shapes and were usually in an agglomerated state, as illustrated in the SEM images. The shape of the particles from the slag releasing was lump-like agglomerates, and background particles were irregularly spherical.

Table 3 lists the elemental compositions of the particles sampled. O, Al, and Si were the predominant elements in the particles collected from the location of slag releasing, while the most abundant background particles were C, O, and Si. Furthermore, the micro elements of particles from the slag releasing location were Na and Fe, which was significantly different from the particles from the background (Zr, Al, Ti).

Table 3. Elemental compositions of ultrafine particles at different sampling sites

Site	Constituent elements (% by mass)
Background	C (36.03), O (43.31), Ca (1.46), Al (0.44), Si (17.46), Zr (0.82), Ti (0.49)
Slag releasing	Al (42.51), O (17.98), Si (24.72), Pt (10.71), Na (3.30), Fe (0.78)

Temporal variations in the total particle concentrations

The temporal variation in total particle concentrations is shown in Figure 3. The total NC, total respirable MC, and SAC during the working activity period were significantly higher than those during the

background and non-activity periods. The highest total NC of the working activity period reached 9.5 × 10^4 pt/cm^3, approximately three times higher than that of the background or non-activity period. The highest SAC of the working activity period was approximately 2700 $\mu m^2/cm^3$, which was about ten times higher than that of the background or non-activity period. The total respirable MC of the working activity period reached 0.52 mg/cm^3, approximately four times higher than that of the non-activity period. The total NC and SAC varied with time, which were influenced by the working activities. The total NC and SAC increased immediately after slag releasing started around 10:52 am and decreased gradually to background level after the operation stopped. The total respirable MC varied withtotal NC, but was delayed for 15 min. Because the enterprise was close to the sea and the blast furnace was in the open air and the ambient wind was relatively strong, the total NC, SAC, and total respirable MC fluctuated greatly even during the non-activity period. Figure 3 (B) shows that personal NC varied with worker activities. The highest personal NC reached a peak of 3 × 10^6 pt/cm^3 at 10:52 am after starting the activity, which was more than 10 times higher than the non-activity period and about 100 times higher than the total NC.

Particle size and size distribution

Figure 4 shows the temporal variations in the mode, median, mean, and geometric sizes of the ultrafine particles from the locations of slag releasing and background. The median, mean, geometric mean, and mode sizes of particles, which were determined using the SMPS, remained relatively stable during the working activity period, ranging from 20 to 50 nm. In contrast, the sizes of particles from the background exhibited significantly greater variations. The changes in the median, mean, geometric mean, and mode sizes of particles during working activity were similar. The variations in particle size monitored by OPS were differentfrom those determined by the SMPS. The various sizes remained relatively steady at the background location; however, there was a certain fluctuation at the slag releasing location. The order of particle sizes by type monitored by SMPS or OPS was as follows: mode < median < geometric mean < mean.

Figure 5 shows a typical particle size distribution (dN/dLogDp, particle/cm^3) as a function of time as measured by SMPS and OPS over a combined range of particle diameters, namely 10.4–96.5 nm for SMPS with the Nano DMA, 103.7–469.8 nm for SMPS with Long DMA, 0.3–10 μm for OPS. The total NC of the particles increased dramatically at approximately 10:50 am when the operation started. Particles released from slag releasing were mainly smaller than 100 nm, and the highest number reached up to 3 × 10^6 pt/cm^3 (Figure 5(A)), which appeared at 10.4 nm and 40 nm. The highest number of particles in the range of 103.7–469.8 nm was about 8 × 10^5 pt/cm^3 (Figure 5(B)), which was much lower than particles smaller than 100 nm. The number of particles greater than 374 nm was lower than 2 × 10^4 pt/cm^3. Large particles were usually present in lower concentrations and with a sharp decrease after the non-activity period, as illustrated in Figure 5(C).

Relationships among the total NC, SAC, and total respirable MC

Figure 3 shows that the variations in the total NC and SAC with the activities were quite similar. Table 2 shows that the order of CR value was: CR_{SAC} (5.39) > $CR_{\text{total NC}}$ (2.87) > CR_{MC} (2.22) at the location of slag releasing. Further, the correlations exhibited in Table 4 shows that there was a significant correlation between the total NC, SAC, and respirable MC. The order of the correlation coefficients (CC) between the total NC, SAC, and respirable MC was $R_{\text{total NC and SAC}}$ (r = 0.681) > $R_{\text{SAC and total respirable MC}}$ (0.456) > $R_{\text{total NC and total respirable MC}}$ (0.424).

Table 4. Correlations between total NC, SAC, and total respirable MC of all samples (n=330)

Variable	Total NC	SAC	Total respirable MC
Total NC (10^4 pt/cm^3)	1.000	-	-
SAC (μm^2/cm^3)	0.681**	1.000	-
Total respirable MC (mg/m^3)	0.424**	0.456**	1.000

**, p<0.01

Discussion

Indoor ultrafine particles from the blast furnace process were collected, and their exposure characteristics were investigated in this study. To our knowledge, this is the first study conducted on detailed exposure characterization for airborne ultrafine particles at a blast furnace in the steelmaking industry using multiple metrics (namely, total NC, total respirable MC, SAC, personal NC, size distribution, morphology, and elemental composition).

The SEM images illustrated the particle size, shape, and state of aggregation. Particles from both the background and blast furnace were irregular agglomerates; however, their shapes were different, which suggested, in part, that the particles were generated from different sources. Simultaneously, the elemental compositions of the particles at the slag releasing location revealed that the dominant elements were O, Al, and Si, while those of background particles were O, C, and Si (Table 3). The characteristic elements of Al and Si at the slag releasing location was supported by a previous study, which revealed that the main components of slag in the steelmaking industry were Al_2O_3 and SiO_2[17]. The differences in the characteristic elements of particles at the two sampling sites further indicated the different particle sources. These findings suggest that steelmaking workers are potentially exposed to these specific ultrafine particles generated from the slag releasing activity. The Al and Si elements, which were found in particles at the slag-releasing location, were also observed in the background particles in a small proportion. A possible explanation for this might be that the particles from the slag releasing process released during the previous working shift diffused to the background location. Thus, the background particles were a mix of outdoor background particles and a small proportion of particlesfrom the slag releasing location. This result was supported by our previous studies on nanoparticles generated from a

nano-Fe_2O_3 manufacturing factory, which reported that the elemental Fe in the nanoparticles from working activities also accounted for a certain proportion of the indoor background particles[23].

The total NC, SAC, and total respirable MC released from the slag releasing location were significantly higher than those from the background or during the non-activity period (Figure 3), which indicated that the slag releasing operation was able to generate higher levels of ultrafine particles. As Figure 3 shows, the total NC and SAC reached a peak at 10:52, while the total respirable MC reached its peak at 11:05 after the period of slag releasing activity. After the activity of slag releasing finished, the total NC and SAC dropped to the background level immediately, while the total MC remained at a high level within the non-activity stage (about 15 min). This finding was supported by our previous study, which demonstrated that respirable MC was not as sensitive as NC and SAC in measuring nanoparticle levels at an automobile manufacturing facility[22]. The temporal variations in the total NC and SAC showed an activity-related characteristic. This result was further confirmed by the variations in the personal NC (Figure 2C). The personal NC increased to the peak rapidly as the working activity started and declined immediately after the end of the working activity. The results of personal sampling showed that the size of the particles decreased from 100 nm to 30 nm as the personal NC increased with working activity and remained smaller than 40 nm even when the personal NC dropped to the background level. The measured location was not equipped with local ventilation, so particles generated from the location of slag releasing could diffuse freely. These results indicated that the working activity had a significant effect on the temporal variations in particle concentrations, which suggested that the monitoring of the airborne particles should be based on the type of working activities[24]. In addition, the concentration curves showed a periodic characteristic which was consisted of a starting phase, a steady-state stage, and a decline phase. This result was supported by Demou et al.[25], who found a similar phenomenon in a metal-based nanoparticle investigation. This performance was also verified by our previous study, which reported that there were activity-related and periodic variations in the NC and SAC of nanoparticles in an Fe_2O_3 manufacturing factory and an automobile manufacturing facility[23, 26].

The mode, median, mean, and geometric size of ultrafine particles remained relatively steady during the background or working activity period (Figure 3). The size of particles based on the SMPS data during the working activity period ranged from 20 to 40 nm, and the background particles ranged from 60 to 120 nm. In contrast to the particles from the slag releasing location, the size variation in the background particles was larger, and the median size was more than 100 nm. The possible reason might be the complicated nature of background particles, as well as the atmospheric conditions. However, the OPS data showed that the larger particles for both the background and blast furnace ranged from 0.3 to 0.4 μm. The size of larger particles from the background remained steady, while the size of particles from the slag releasing location exhibited several peaks. The maximum size of the particles from the slag releasing could reach approximately 0.8 μm, which suggests that the particles released from the slag releasing location could quickly aggregate into large particles.

Particle size distribution showed that particles released from the slag releasing location were mainly smaller than 100 nm, and the highest number concentration appeared at 10.4 nm and 40 nm, which was as high as 3.5×10^6 pt/cm^3 (Figure 4). The total NC of particles less than 100 nm was approximately 10 times higher than that of particles above 100 nm. This result provided direct evidence that most of the particles released from the slag releasing location were nanoparticles. The density of slag in this process was approximately 7,900 kg/m^3, and the average NC of particles with sizes less than 100 nm (10.4–96.5 nm) reached 2×10^6 pt/cm^3, which was 100 times larger than the exposure limit of 2×10^4 pt/cm^3 for nanomaterials with a density > 6,000 kg/m^3 recommended by the Institute for Occupational Safety and Health of the German Social Accident Insurance[27]. However, the total MC observed was only 0.2 mg/m^3, which was still much lower than the occupational exposure limit of other dust (8 mg/m^3) in China[28]. Furthermore, particles were distributed widely and evenly in this workplace for a long time due to a lack of ventilation. Our data on personal NC and total NC indicated that workers were exposed to high NC or SAC levels of ultrafine particles generated by the slag releasing activity, and the total respirable MC was no longer an appropriate evaluation metric for ultrafine particles. This was confirmed by a previous study on airborne nanoparticles in a wire electrical discharge matching workshop, which found that the total NC of nanoparticles was 100 times higher than the exposure limit, and provided an evaluation of the potential exposure limits of associated metal nanoparticles[29].

The relationships among total NC, SAC, and total respirable MC were determined based on the following parameters: consistency of temporal variation in particle concentrations, CR, and CC. The temporal variation in the total NC and SAC was dependent on working activities (Figure 3A). The change in total respirable MC was followed by the change in working activities (Figure 2B). The CR values for the three metrics were CR_{SAC} (5.39) > $CR_{total\ NC}$ (2.87) > $CR_{respirable\ MC}$ (2.22) (Table 2). Correlation analysis showed that there was a significant correlation among the total NC, SAC, and respirable MC. The order of CC between the total NC, SAC, and respirable MC was $R_{total\ NC\ and\ SAC}$ ($r = 0.681$) >$R_{SAC\ and\ respirable\ MC}$ (0.456) >$R_{total\ NC\ and\ respirable\ MC}$ (0.424) (Table 4). These findings indicated that the total NC and SAC were more appropriate metrics for characterizing particles at the slag releasing location than total respirable MC.

The likely association between NC and MC has been investigated in several studies. Sajedifar et al. reported that there was no agreement between number and mass concentration, and as the particles' size became smaller, their mismatch became more apparent[30]. Zhu et al.[31] observed that the NC and MC showed a positive correlation, but the coefficients of determination (R2) of linear regression, logarithmic curve, polynomial, power function, and exponential curve model were relatively low, which indicates that there is no fixed regression relationship between the two concentrations, and neither is a definite coefficient that can be used to convert each other. Data on the correlation among the three metrics are limited for engineered nanoparticles, especially metal nanoparticles. Chung et al. reported that SAC and NC were highly correlated, and NC and MC had a moderate positive association[32], which was confirmed in our previous study about Fe_2O_3 nanoparticles released from a manufacturing facility[23]. In our

preliminary study on nanoparticles generated from gas metal arc welding, we found that the MC was not as sensitive as NC or SAC[26]. Furthermore, we examined the relationship among the NC, SAC, and MC of nanoparticles in workplaces, and found that respirable MC was less sensitive than NC or SAC to levels of exposure to different nanoparticles. The CC order of the three exposure metrics for nanoparticles was: $R_{SAC\ and\ NC} > R_{SAC\ and\ MC} > R_{NC\ and\ MC}$[33]. In brief, the NC and SAC metrics are significantly distinct from the MC in characterizing exposure to nanoparticles.

Because different instruments were employed in this study to characterize the particles during the blast furnace process, it is necessary to clarify that these measurements may have some disagreement[34]. The discrepancy between data from different instruments might be the result of the following reasons: (1) the size range of instruments is different (10.4–487 nm for SMPS, 300–1000 nm for OPS, < 700 nm for DiSCmini); (2) the principles of detection are different (electrical mobility diameter for SMPS, light scattering equivalent diameter for OPS), and (3) particle sedimentation, aggregation, and coagulation may occur. In addition, with the limitation of instruments, the background and workplace particles cannot be monitored simultaneously. Therefore, the result is probably influenced by wind, anthropogenic factors, and others.

Conclusions

In summary, based on the above findings, conclusions can be drawn as follows: (1) metal elements were the dominant component of indoor particles released from the slag releasing; (2) variations in particle concentrationsdisplayed activity-related and periodic characteristics; (3) most of the particles released from the slag releasing location were smaller than 100 nm, and the highest NC appeared at 10.4 and 40 nm, the median, mean, geometric mean, and modal sizes of particles ranged from 20 to 50 nm during the slag releasing activities; (4) total NC and SAC metrics are more appropriate for characterizing indoor ultrafine particles at the slag releasing location than total respirable MC.

In the steelmaking industry, it is necessary to adopt specific approaches to protect workers' healthas they are occupationally exposed to high levels of ultrafine particles. This study provides baseline data on the exposure characteristics of indoor particles during blast furnace operations. These data can be used to develop guidance for ultrafine particle exposure assessment in workplaces such as blast furnaces, and for further studies on the biological relevance of exposure-related metrics or health risks. More studies are needed to better understand the exposure characteristics in the steelmaking industry.

Abbreviations

CC: correlation coefficient

CPC: concentration particle counter

CR: concentration ratio

DMA: differential mobility analyzer

MC: mass concentration

NC: number concentration

OPS: optical particle sizer

SAC: surface area concentration

SMPS: scanning mobility particle sizer

Declaration

Ethics approval and consent to participate

Not applicable.

Consent for publication

Not applicable.

Availability of data and materials

The datasets used in the current study are available from the corresponding author on reasonable request.

Declaration of interests

The authors declare that they have no competing interests.

Funding

This work was supported by the Medical Health Technology Project by the Health Commission of Zhejiang (No. 2020KY517 and 2018KY332), and the reform and development program from Beijing Municipal Institute of Labor Protection in 2020, and the NaturalScience Foundation of China (81472961).

Authors’ contribution

Xiangjing Gao: Investigation, funding acquisition, and writing original draft preparation.

Hua Zou: Investigation and funding acquisition.

Qunli Wang: Resources

Zanrong Zhou: Project administration

Weiming Yuan: Visualization

Yuqing Luan: Supervision

Quanchang Jian: Supervision

Meibian Zhang: Conceptualization, writing, review, and editing.

Shichuan Tang: Conceptualization

All authors read and approved the final manuscript.

Acknowledgements

The authors would like to acknowledge the steelmaking industry and relevant staff.

Authors' email addresses

Xiangjing Gao: xjgao@cdc.zj.cn

Hua Zou: hzou@cdc.zj.cn

Qunli Wang: 51296651@qq.com

Zanrong Zhou: zrzhou@cdc.zj.cn

Weiming Yuan: wmyuan@cdc.zj.cn

Yuqing Luan: yqluan@cdc.zj.cn

Quanchang Jian: cjquan@cdc.zj.cn

Meibian Zhang: mbzhang@cdc.zj.cn

Shichuan Tang:tsc3496@sina.com

References

1. Worldsteel. Worldsteel Short Range Outlook June 2020. 2020. https://www.worldsteel.org/media-centre/press-releases/2020/worldsteel-short-range-outlook-june-2020.html. Accessed 04 June 2020.

2. Wang, K, Wang, C, Lu, X, and Chen, J. Scenario analysis on CO2 emissions reduction potential in China's iron and steel industry. Energ Policy, 2007; 35, (4): 2320-2335.

3. WorldsteelAssociation. March 2019 crude steel production. 2019. https://www.worldsteel.org/media-centre/press-releases/2019/March-2019-crude-steel-production.html. Accessed 29 April 2019.

4. Ogundele L T, Owoade O K, Hopke P K, and Olise FS. Heavy metals in industrially emitted particulate matter in Ile-Ife, Nigeria. Environ Res, 2017; 156: 320-325.

5. Liu W, Xu Y, Zhao Y, Liu Q, Yu S, Liu Y, Wang X, Liu Y, Tao S, and Liu W. Occurrence, source, and risk assessment of atmospheric parent polycyclic aromatic hydrocarbons in the coastal cities of the Bohai and Yellow Seas, China. Environ Pollut, 2019; 254, (Pt B): 113046.

6. Liu Q, Lu Z, Xiong Y, Huang F, Zhou J,and Schauer J J. Oxidative potential of ambient PM2.5 in Wuhan and its comparisons with eight areas of China. Sci Total Environ, 2020; 701: 134844.

7. Li M, Liu H, Geng G, Hong C, Liu F, Song Y, Tong D, Zheng B, Cui H, Man H. Anthropogenic emission inventories in China: a review. Nat Sci Rev, 2017; 4, (6): 834-866.

8. National Bureau of Statistics. Dust (soot) emission (tons). http://www.stats.gov.cn/. Accessed 4 July 2019.

9. Sasi B M J. Air pollution caused by iron and steel plants. Intern J Min, Metal & Mech Eng (IJMMME), 2013; 1, (3):219-222.http://www.isaet.org/images/extraimages/P513673.pdf.

10. Brown L M, Collings N, Harrison R M, Maynard A D, and Maynard R L. Ultrafine particles in workplace atmospheres - Discussion.2000; 358: 2673-2682.

11. Hutchison G R, Brown D M, HibbsL R, Heal M R, Donaldson K, Maynard R L, Monaghan M, Nicholl A,and Stone V. The effect of refurbishing a UK steel plant on PM10 metal composition and ability to induce inflammation. Respir Res, 2005; 6, (1):1-16.

12. Ito K, Christensen W F, Eatough D J, Henry R C, Kim E, Laden F, Lall R, Larson T V, Neas L, Hopke P K,and Thurston G D. PM source apportionment and health effects: 2. An investigation of intermethod variability in associations between source-apportioned fine particle mass and daily mortality in Washington, DC. J Exposure Sci Environ Epidem, 2006; 16, (4): 300-310.

13. Chang E E, Wei-Chi W, Li-Xuan Z,and Hung-Lung C. Health risk assessment of exposure to selected volatile organic compounds emitted from an integrated iron and steel plant. Inhal Toxicol, 2010; 22 (2): 117-125.

14. Wang K, Tian H, Hua S, Zhu C, Gao J, Xue Y, Hao J, Wang Y,and Zhou J. A comprehensive emission inventory of multiple air pollutants from iron and steel industry in China: Temporal trends and spatial variation characteristics. Sci Total Environ, 2016; 559: 7-14.

15. Zhou X, Strezov V, Jiang Y, Yang X, Kan T,and Evans T. Contamination identification, source apportionment and health risk assessment of trace elements at different fractions of atmospheric particles at iron and steelmaking areas in China. PloS one, 2020; 15, (4): e0230983.

16. Lanzerstorfer C. Characterization of dust from blast furnace cast house de-dusting. Environ Tech, 2017; 38, (19): 2440-2446.

17. Fan Z Z, Zhao Y L, Zhao H N, Liang X Y, Sun J W, Wang B G,and Wang Y J. Emission characteristics of PM2.5 from blast furnace iron making [Article in Chinese].Huan Jing Ke Xue, 2014; 35, (9): 3287-3292.

18. Jarvela M, Huvinen M, Viitanen A K, Kanerva T, Vanhala E, Uitti J, Koivisto A J, Junttila S, Luukkonen R, and Tuomi T. Characterization of particle exposure in ferrochromium and stainless steel production. J Occup Environ Hyg, 2016; 13, (7): 558-68.

19. MSeipenbusch, ABinder, GKasper. Temporal evolution of nanoparticle aerosols in workplace exposure. Ann Occup Hyg, 2008; 52, (8): 707-716.

20. Jian L, Zhu Y P, Zhao Y. Monitoring fine and ultrafine particles in the atmosphere of a Southeast Chinese city. J Environ Monit, 2011; 13, (9): 54-60.

21. Gao X, Zou H, Xu X, Zhou L, Tang S, Yuan W,and Zhang M. Developing a guideline for measuring the total number concentration of engineering nanomaterials in workplaces in China. J Occup Health, 2019; 61, (2): 197-202.

22. Zhang M, Jian L, Bin P, Xing M, Lou J, Cong L, Zou H. Workplace exposure to nanoparticles from gas metal arc welding process. J Nanoparticle Res, 2013; 15, (11): 1-14.

23. Xing M, Zhang Y, Zou H, Quan C, Chang B, Tang S, Zhang M. Exposure characteristics of ferric oxide nanoparticles released during activities for manufacturing ferric oxide nanomaterials. Inhal Toxicol, 2015; 27, (3): 138-48.

24. Methner M, Beaucham C, Crawford C, Hodson L,and Geraci C. Field application of the Nanoparticle Emission Assessment Technique (NEAT): task-based air monitoring during the processing of engineered nanomaterials (ENM) at four facilities. J Occup Environ Hygiene, 2012; 9, (9): 543-55.

25. Evangelia D, Philippe P, and Stefanie H.Exposure to manufactured nanostructured particles in an industrial pilot plant. Ann Occup Hyg, 2008; 52, (8): 695-706.

26. Zhang M, Jian L, Bin P, Xing M,and Zou H. Workplace exposure to nanoparticles from gas metal arc welding process. J Nanoparticle Res, 2013; 15: 2016.

27. IFA. Criteria for assessment of the effectiveness of protective measures.2020. https://www.dguv.de/ifa/fachinfos/nanopartikel-am-arbeitsplatz/beurteilung-von-schutzmassnahmen/index-2.jsp.

28. National Health Commission of the People's Republic of China. Occupational exposure limits for hazardous agents in the workplace: In Chemical hazardous agents. GBZ 2.1-2019. 2019.

http://www.nhc.gov.cn/wjw/pyl/202003/67e0bad1fb4a46ff98455b5772523d49.shtml. Accessed 03 March 2020.

29. ChenR, Shi X F, Bai R, Rang W, Huo L L, Zhao L, Long D X, David Y H Pui,and Chen C Y. Airborne Nanoparticle Pollution in a Wire Electrical Discharge Machining Workshop and Potential Health Risks. Aerosol Air Qual Res, 2015; 15, (1): 284-294.

30. Sajedifar J, Kokabi A H, Azam K, Farhang S, Karimi A, and Golbabaei F. The comparative assessment of welders' exposure to welding fumes based on mass concentration and number concentration. Journal of Health and Safety at Work, 2016; 6, (4): 17-26.

31. Zhu X, Li T,and Wang H. Relationship between dust mass concentration and fiber number concentration of refractory ceramic fibers [Article in Chinese]. Chinese journal of industrial hygiene and occupational diseases, 2015; 33, (4): 309-312, .

32. Chung EK, Jang JK, Song SW,and Kim J. Relationships between a Calculated Mass Concentration and a Measured Concentration of PM 2.5 and Respirable Particle Matter Sampling Direct-Reading Instruments in Taconite Mines. J Korean Society of Occup and Environ Hygiene, 2014; 24, (1): 65-73.

33. Zou H, Zhang Q, Xing M, Gao X, Zhou L, Tollerud D J, Tang S,and Zhang M. Relationships between number, surface area, and mass concentrations of different nanoparticles in workplaces. Environ Sci: Proc Impact, 2015; 17, (8): 1470-81.

34. Frank E P , Dhimiter B, Gilbert H, Ji-Young P, Maria P, Jon McCarthy, Kristin L B, Axel F, Yongho J, M A V, George G, and Mark D H. Characterization of exposure to airborne nanoscale particles during friction stir welding of aluminum. Ann Occup Hyg, 2010; 54 (5): 486-503.

Figures

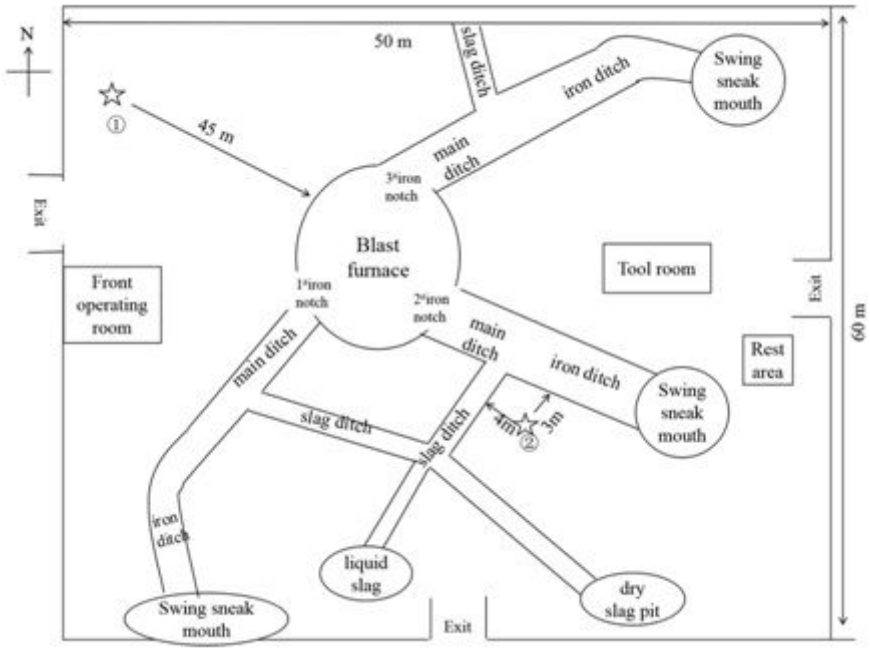

Figure 1

Workshop layout and sampling locations marked with an asterisk. Sampling ①: background; ②: slag releasing.

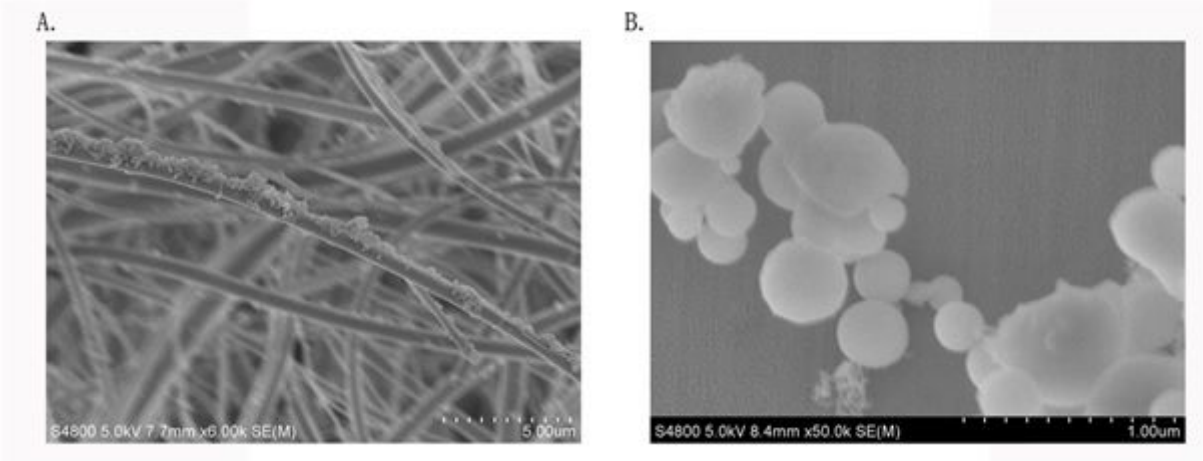

Figure 2

Scanning electron micrographs of particles from the locations of slag releasing and background. (a) lump-like agglomerates of ultrafine particles at the slag releasing location; (b) irregular spherical ultrafine particles from the background.

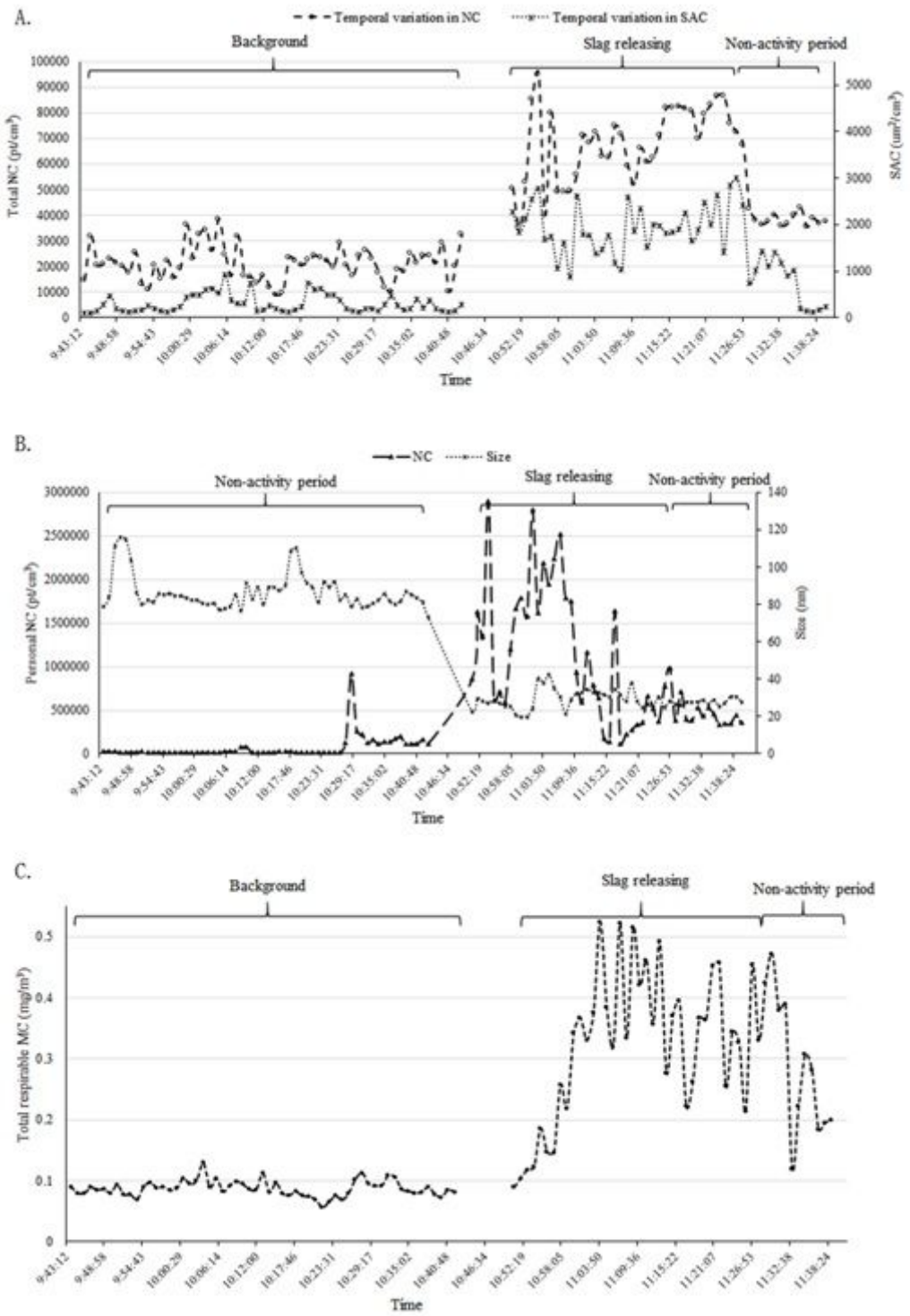

Figure 3

Temporal variations in total particle concentrations associated with working activities. (A) Temporal variations in total NC and SAC at background and operation locations. (B) Temporal variations in personal NC and its size during the working and non-activity periods. (C) Temporal variations in total respirable MC at the background and operation location.

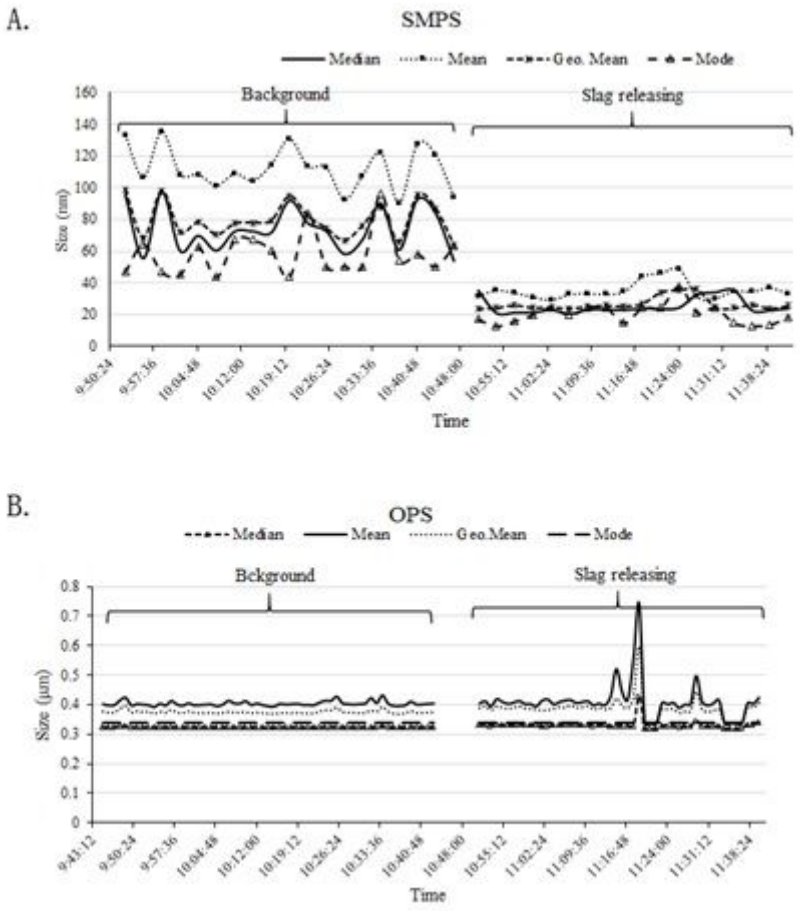

Figure 4

Temporal variations in mode, median, mean, and geometric mean particle sizes. (A) Mode, median, mean, and geometric mean size of particles monitored by SMPS at background and operation location. (B) Mode, median, mean, and geometric mean size of particles monitored by OPS at background and operation locations.

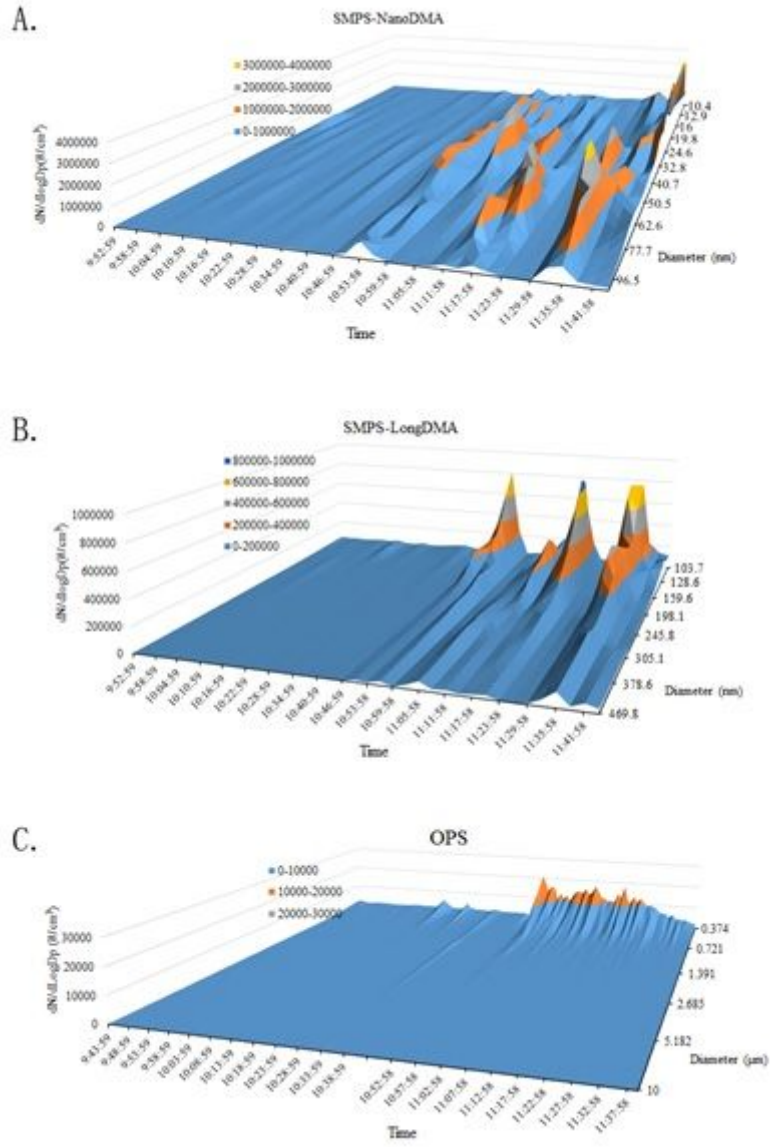

Figure 5

Real-time particle size spectrum. (A) SMPS with Nano DMA; (B) SMPS with Long DMA; (C) OPS. Most of the particles were smaller than 100 nm, and the highest number reached 3 × 106 pt/cm3 at 10.4 nm and 40 nm.